NEUROLOGICAL RESEARCH
2021, VOL. 43, NO. 7, 595–607
https://doi.org/10.1080/01616412.2021.1902702

Taylor & Francis
Taylor & Francis Group

ORIGINAL RESEARCH PAPER

A Cortical Parcellation Based Analysis of Ventral Premotor Area Connectivity

John R. Sheets[a], Robert G. Briggs[a], Nicholas B. Dadario[b], Isabella M. Young[c], Michael Y. Bai[d], Anujan Poologaindran[e], Cordell M. Baker[a], Andrew K. Conner[a] and Michael E. Sughrue[d]

[a]Department of Neurosurgery, University of Oklahoma Health Sciences Center, Oklahoma City, Oklahoma, USA; [b]Robert Wood Johnson Medical School, Rutgers University, New Brunswick, New Jersey, USA; [c]Cingulum Research, Cingulum Health, Sydney, Australia; [d]Department of Neurosurgery, Centre for Minimally Invasive Neurosurgery, Prince of Wales Private Hospital, Sydney, Australia; [e]Brain Mapping Unit, University of Cambridge, Cambridge, UK

ABSTRACT

Introduction. The ventral premotor area (VPM) plays a crucial role in executing various aspects of motor control. These include hand reaching, joint coordination, and direction of movement in space. While many studies discuss the VPM and its relationship to the rest of the motor network, there is minimal literature examining the connectivity of the VPM outside of the motor network. Using region-based fMRI studies, we built a neuroanatomical model to account for these extra-motor connections.

Methods. Thirty region-based fMRI studies were used to generate an activation likelihood estimation (ALE) using BrainMap software. Cortical parcellations overlapping the ALE were used to construct a preliminary model of the VPM connections outside the motor network. Diffusion spectrum imaging (DSI)-based fiber tractography was performed to determine the connectivity between cortical parcellations in both hemispheres, and a laterality index (LI) was calculated with resultant tract volumes. The resulting connections were described using the cortical parcellation scheme developed by the Human Connectome Project (HCP).

Results. Four cortical regions were found to comprise the VPM. These four regions included 6v, 4, 3b, and 3a. Across mapped brains, these areas showed consistent interconnections between each other. Additionally, ipsilateral connections to the primary motor cortex, supplementary motor area, and dorsal premotor cortex were demonstrated. Inter-hemispheric asymmetries were identified, especially with areas 1, 55b, and MI connecting to the ipsilateral VPM regions.

Conclusion. We describe a preliminary cortical model for the underlying connectivity of the ventral premotor area. Future studies should further characterize the neuroanatomic underpinnings of this network for neurosurgical applications.

ARTICLE HISTORY
Received 17 August 2020
Accepted 10 March 2021

KEYWORDS
Connectomics; ventral premotor; VPM; tractography; parcellation

Introduction

The Ventral Premotor Area (VPM) is responsible for coordinating various aspects of everyday actions in humans [1]. It has been demonstrated to have a role in finger placement and grip strength determination when lifting an object [2–15]. Specifically, the VPM is believed to relay information about the geometrical shape of an object to the Primary Motor Cortex to facilitate more specific finger placement for optimal grasp [7]. If a lesion is placed between Dorsal Premotor Area (DPM) and VPM, the subject will be unable to perform the complex distal hand and finger movements required to securely grasp and lift an object [4]. Additionally, the VPM is highly active in action observation/imitation [16–19] and it is suggested that it could play a role in the basis of human language acquisition [18].

While these previously mentioned studies do present a clear picture of functional connections and the associated activity of the VPM, no studies yet have shown a detailed anatomical map of the VPM and its complete cortical projections. A detailed map of VPM projections could be a key tool in future research studies, aiding in the identification of specific white matter tracts. Additionally, such a map could also be useful in the analysis of tumor patients for surgical intervention by serving as a guide for useful regions to preserve, if possible.

In this study, we constructed a model of the VPM based on the cortical parcellation scheme published from the Human Connectome Project (HCP) [20]. Using relevant task-based functional magnetic resonance imaging (fMRI) studies and BrainMap (http://www.brainmap.org/), a collection of open-access software programs used to generate activation likelihood estimations (ALEs) from fMRI studies, we have identified the key cortical areas involved in the VPM [21,22]. After identifying these regions of interest, we performed diffusion spectrum imaging (DSI)-based tractography to determine the structural connectivity between parcellations, both within the VPM and its

CONTACT Michael E. Sughrue sughruevs@gmail.com Centre for Minimally Invasive Neurosurgery, Prince of Wales Private Hospital, Suite 19, Level 7, Randwick, NSW 2031.

connections to other areas of the cortex. Our goal is to provide a more detailed anatomic model of the VPM and its outside connections for use in future studies.

Methods

Sleuth literature search

We utilized Brainmap Sleuth to perform a search in July 2017. Studies were selected for meta-analysis if they mapped the Ventral Premotor Area (The Brainmap Functional Papers database includes over 3000 papers that use functional imaging to measure task-dependent brain activity to relate cognitive functions to brain regions; www. brainmap.org).

The database search was carried out based on brain region as opposed to function for the reason that it would be difficult to isolate the VPM in a motor-based task without picking up numerous other regions in the process [23–26]. Only studies utilizing healthy subjects were utilized. This search revealed 32 studies focusing on the Ventral Premotor Area each with specific foci mapped [13,14,27–56].

GingerALE meta-analysis

All foci for the search were exported in Talaraich space as a GingerALE text file. Brainmap GingerALE was used to perform ALE meta-analyses on the foci generated from the Sleuth search using Talaraich coordinate space and the recommended settings for Cluster-Level Interference found in the GingerALE manual: Single Study, Coordinate System: Talaraich, Cluster Level 0.05, Permutations = 1000, Uncorrected P = 0.001. Cluster-Level Interference is a thresholding algorithm in the GingerALE software that finds contiguous volumes above a minimum 'cluster-forming threshold' using FDR or an uncorrected P-value and tracks the distribution of their volume (brainmap.org). The Cluster-Level Interference algorithm then generates simulated data clusters such that only a small percentage (in our case: Cluster Level = 5%) of the simulated data clusters may exceed the threshold.

Matching of parcellations to literature search ROIs

The NIFTI file generated by GingerALE was opened in Brainmap's Mango as an overlay on Mango's default 3D brain 'sample image'. Parcellations from Glasser's 2016 study that had previously been converted to MNI NIFTI Region of Interests (ROIs) were overlaid and converted to Talaraich Space coordinates [20]. 3D Images of Glasser Parcellation ROIs overlapping with the Semantic ROIs were generated using Mango's Surface function. A parcellation was determined to 'match' a literature search ROI if it could be visually observed to overlap with the region when viewed sagittally, coronally, and axially. Parcellations that only touched ROI edges were excluded.

Tractography

Fiber tractography was done in DSI Studio (http://dsi-studio.labsolver.org) using publicly available imaging data from the Human Connectome Project (HCP) (http://humanconnectome.org, release Q3). Diffusion studies from the HCP utilized a customized Siemens 3T Skyra scanner (G_{max} = *100 mT/m*) to study 1200 subjects as described previously [20,57]. Tractography in this study was performed individually with 25 randomly chosen adult subjects. A multi-shell diffusion scheme was used, and the b-values were 990, 1985, and 2980 s/mm^2. The number of diffusion sampling directions was 90, 90, and 90, respectively. The in-plane resolution was 1.25 mm. The slice thickness was 1.25 mm. The diffusion data were reconstructed using generalized q-sampling imaging with a diffusion sampling length ratio of 1.25 [58].

Laterality indices (LI) were calculated based on the average volume of major tracts identified using the formula (Right average tracts – Left average tracts)/(Right average tracts + Left average tracts) [59]. A Shapiro-Wilk test for normality was performed on all data and paired Wilcoxon signed-rank tests with continuity correction were utilized to assess differences between cerebral hemispheres for major tracts ($p \leq 0.05$).

Results

ALE regions and their corresponding parcellations

Figure 1 shows the ALE of the 30 region-based fMRI experiments included in our meta-analysis. Both right and left cerebral hemispheres were included in this analysis to account for possible cerebral differences within individuals. Four regions of interest were identified which overlapped the fMRI data. The four regions include6v, 4, 3b, and 3a. Comparison overlays between the cortical parcellations and the ALE are shown in Figure 2.

Structural connectivity of the VPM

Tractography was utilized to determine the basic structural connectivity of VPM. These results are shown in Table 1 and Figure 4 through Figure 7. The connections found consistently across all 25 subjects included in our analysis are summarized in Figure 3. It was found that area 3a has ipsilateral connections with 6a, 6d, and 6r (Figure 4).

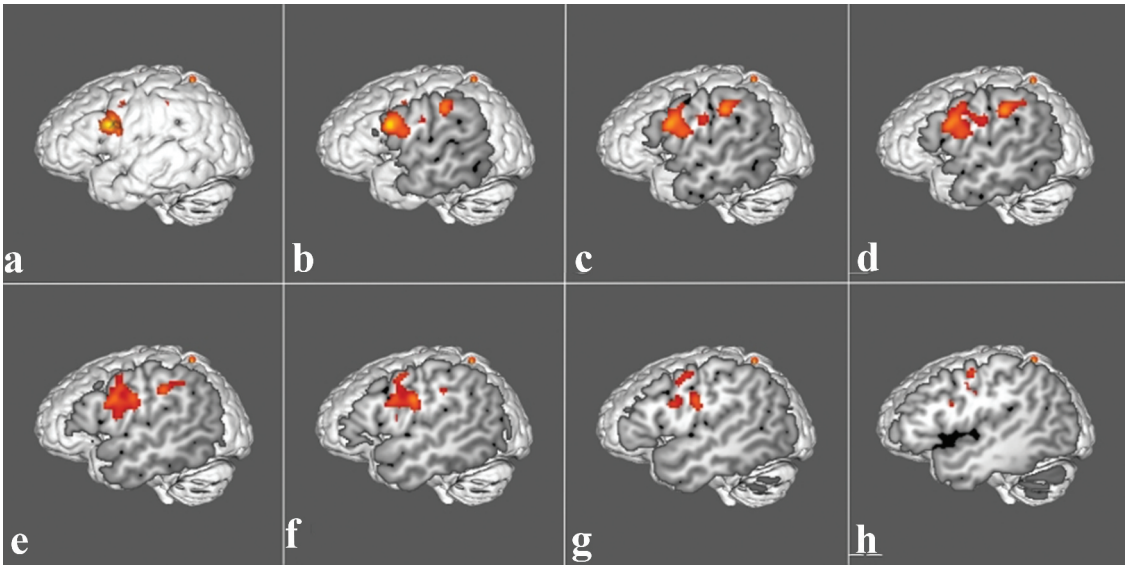

Figure 1. Representative sagittal images on a sample MNI brain showing the ALEs in the study. Colored pixels represent significant ALE values with lighter colors representing higher ALE values.

Area 3b has ipsilateral connections with premotor areas FEF, 55b, and 6r (Figure 5). Area 4 has ipsilateral connections with premotor areas FEF, 55b, 6r, 6d, and 6a. Additionally, area 4 showed contralateral connections to premotor areas FEF and 55b (Figure 6). Furthermore, areas 3a, 3b, and 4 showed contralateral VPM counterparts, with areas 3a, 3b, and 4 on the contralateral side. A schematic showing the average number of tracts is shown in Figure 8.

Significant rightward lateralization was demonstrated in all VPA regions of interest with tracts connecting to area 1 on the ipsilateral side ($p < 0.05$ for area 4, 6v, 3b, and 3a). Connections between area 55b and 6v were lateralized to the right as well as area 3a and MI to the left. The connections of area 4 with its analog on the contralateral side were found to be lateralized to the right (Table 1).

Discussion

In this study, we utilized meta-analytic software and deterministic tractography to construct a preliminary model of the VPM and its connections throughout the human cortex. We aim to create a more specific anatomical map of not only the VPM but also its projections both ipsilaterally and contralaterally to be used in future studies. Here we will present an analysis of the parcellations described in our model and their cortical projections. Included is some basic information on the function of each of the general areas projected from the VPM, to encourage discussion on the possible reason is for the consistent anatomical connections.

Premotor cortex

As expected, the VPM and its associated parcellations show extensive connections with areas deemed to be within the more classic interpretation of the premotor area. The premotor cortex has long been associated with its ability to facilitate movement [60] and plays a significant role in the actions attributed to VPM. Considering VPM activity has been demonstrated in language acquisition, the connections observed between VPM, 55b, and 6r are consistent with those findings [17]. 55b and 6r are two areas that have been classically associated with numerous language function activities [61,62]. Additionally, area FEF is known to function in visual attention processes [63], an action likely critical for the VPM action observation/imitation functions [15–18]. These connections likely provide anatomical reasoning for these functional associations.

Interestingly, the ipsilateral connection between area 55b and 6v were found to be lateralized to the right. Area 55b is an area recently thought to be involved in language processing and is asymmetrical between hemispheres [20]. In the left hemisphere, area 55b associates with the DMN network system while it associates with the Salience network on the right. Given that area 6v is part of the Salience network in both cerebral hemispheres, it is interesting to speculate that our data showing a lateralized connection between 55b and 6v offer an opportunity to further study a possible mechanism for the different network affiliations between hemispheres for area 55b.

Inferior Frontal Gyrus and Middle Frontal Gyrus

Area 3a of VPM demonstrated connections to Middle Frontal Gyrus (MFG) areas 8AV and 8BL.

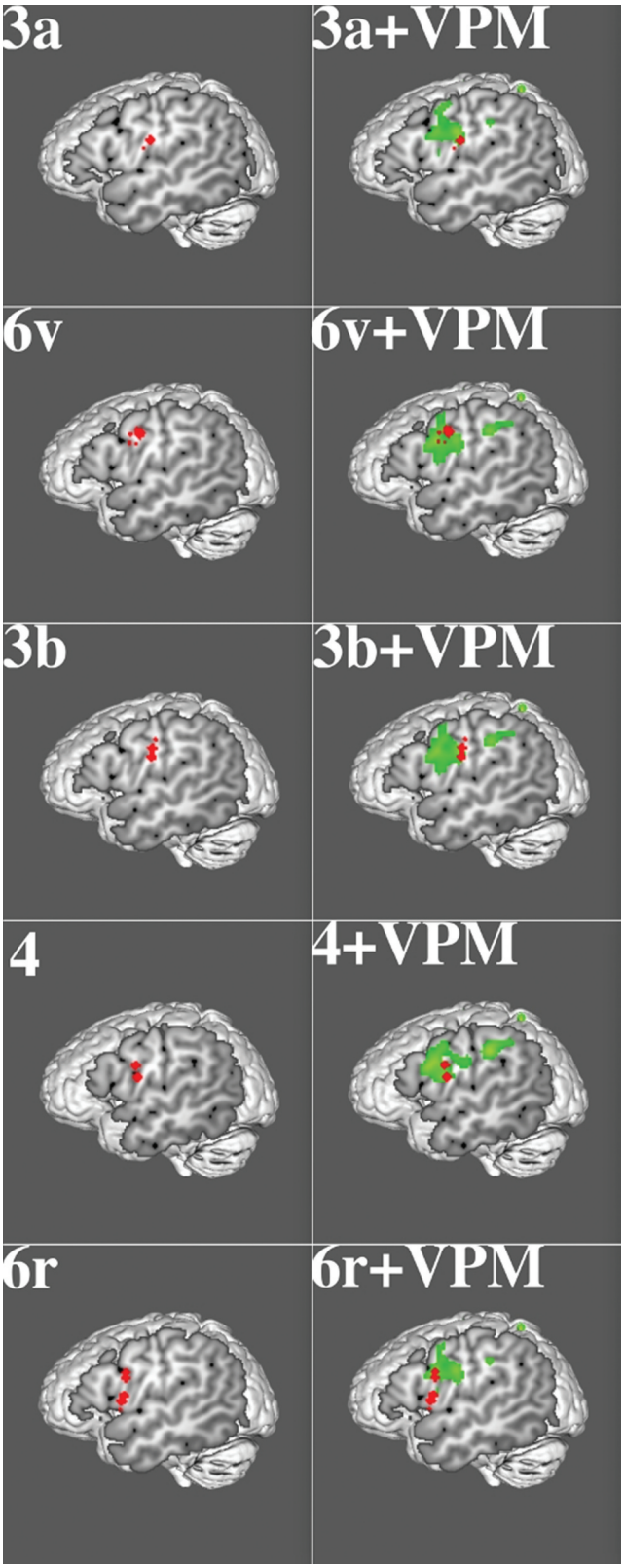

Figure 2. Comparison overlay images between cortical parcellation (green) with ALE data (red).

Additionally, area 4 of VPM also demonstrated connections to MFG area 8AV and Inferior Frontal Gyrus area 8C. The MFG and IFG have both been implicated in aspects of executive function including action selection, action inhibition, and verbal fluency/processing [64–67]. Executive function abilities are a large part of the actions attributed to VPM such as finger placement based on the geometrical shape and grip strength when lifting an object. Additionally, the language acquisition aspect of VPM could also be contributed to by the connections to IFG and MFG observed here [2–15,18].

Table 1. Type and average strength of connection in the VPM network. Connections from the VPM network were measured with regions on both the ipsilateral and contralateral hemispheres. A lateralization index was calculated as (Right average tracts – Left average tracts)/(Right average tracts + Left average tracts). Negative values indicate a leftward asymmetry and positive values a rightward asymmetry. Paired Wilcoxon signed-rank tests with continuity correction were calculated with 95% confidence intervals between left hemispheric tracts and right hemispheric tracts between individuals.

		4		6v		3b		3a	
Ipsi-lateral	**6d**	1456.36	LI = −0.12 (p = 0.210)	7.96	LI = −0.78 (p = 0.281)	674	LI = 0.02 (p = 0.647)	464.76	LI = −0.28 (p = 0.247)
	6r	476.36	LI = −0.27 (p = 0.592)	1834.24	LI = 0.06 (p = 0.474)	172.84	LI = −0.64 (p = 0.157)	124.08	LI = −0.14 (p = 0.306)
	8AV	120.76	LI = −0.19 (p = 0.590)	79.4	LI = −0.26 (p = 0.435)	48.24	LI = −0.59 (p = 0.126)	26.36	LI = −0.16 (p = 0.675)
	8BL	141.48	LI = 0.51 (p = 0.944)	4.56	LI = −0.12 (p = 0.888)	24.56	LI = −0.24 (p = 0.834)	18.56	LI = 0.23 (p = 0.529)
	PFt	316.52	LI = −0.17 (p = 0.987)	41.84	LI = −0.29 (p = 0.937)	620.92	LI = −0.09 (p = 0.374)	125.88	LI = 0.27 (p = 0.603)
	MI	112.16	LI = −0.76 (p = 0.701)	16.32	LI = −0.08 (p = 1.000)	78.24	LI = −0.79 (p = 0.056)	51.2	LI = −0.89 (p = 0.013)*
	Lipd	31.6	LI = −0.78 (p = 0.067)	2.8	LI = −1.00 (p = 1.000)	54.8	LI = −0.17 (p = 0.706)	20.68	LI = −0.58 (p = 0.151)
	IP1	50.8	LI = 0.30 (p = 0.834)	2.88	LI = −1.00 (p = 1.000)	74.6	LI = 0.31 (p = 0.722)	18	LI = 0.39 (p = 1.000)
	AIP	216.12	LI = −0.23 (p = 0.484)	18.84	LI = 0.07 (p = 0.554)	334.16	LI = −0.23 (p = 0.843)	57.56	LI = −0.09 (p = 0.472)
	PFm	155.72	LI = −0.15 (p = 0.195)	20.2	LI = 0.10 (p = 0.529)	112.4	LI = −0.45 (p = 0.158)	48.8	LI = 0.03 (p = 1.000)
	1	1689.24	LI = 0.10 (p = 0.026)*	172.72	LI = 0.24 (p = 0.043)*	4419.48	LI = 0.13 (p = 0.026)*	876.68	LI = 0.06 (p = 0.011)*
	55b	790.88	LI = −0.01 (p = 0.263)	404.48	LI = 0.25 (p = 0.006)**	639.24	LI = −0.07 (p = 0.578)	170.84	LI = −0.35 (p = 0.256)
	FEF	1253.64	LI = 0.39 (p = 0.101)	62.28	LI = −0.43 (p = 0.660)	578.96	LI = −0.03 (p = 0.259)	173.8	LI = −0.55 (p = 0.033)
	8C	133.52	LI = 0.17 (p = 0.433)	334.32	LI = −0.19 (p = 0.679)	64.36	LI = −0.36 (p = 0.067)	34.4	LI = 0.00 (p = 0.799)
Contra-lateral	**4**	883.44	LI = 0.13 (p = 0.006)**	10.64	LI = 0.17 (p = 1.000)	176.72	LI = 0.14 (p = 0.660)	154.04	LI = 0.00 (p = 0.328)
	3a	122.52	LI = 0.37 (p = 0.889)	1.16	LI = 0.66 (p = 0.414)	19.88	LI = 0.09 (p = 0.400)	4.68	LI = 0.33 (p = 0.174)
	3b	119.32	LI = 0.13 (p = 0.616)	4	LI = 1.00 (p = 0.371)	102.2	LI = −0.07 (p = 0.155)	12.32	LI = 0.12 (p = 0.888)
	FEF	25.64	LI = 0.35 (p = 1.000)	5.84	LI = −1.00 (p = 0.371)	2.88	LI = −1.00 (p = 0.371)	0.32	LI = −1.00 (p = 1.000)
	55b	21.8	LI = 0.29 (p = 0.590)	0.24	LI = −1.00 (p = 0.371)	3.92	LI = −1.00 (p = 1.000)	1.12	LI = −0.14 (p = 1.000)

LI, lateralization index. *p < 0.05 **p < 0.01

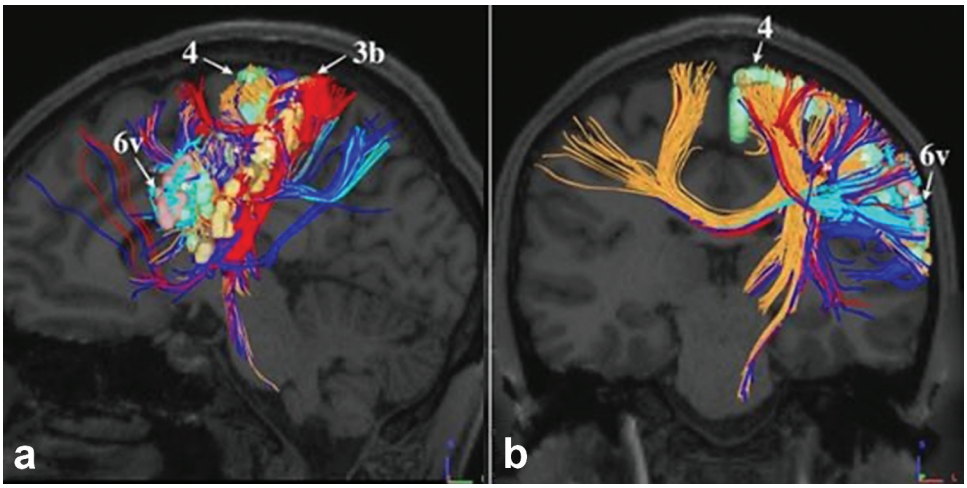

Figure 3. Diffusion tractography in sagittal and coronal planes showing all parcellations and basic model of the VPM. Different colors represent unique fiber bundle tracts.

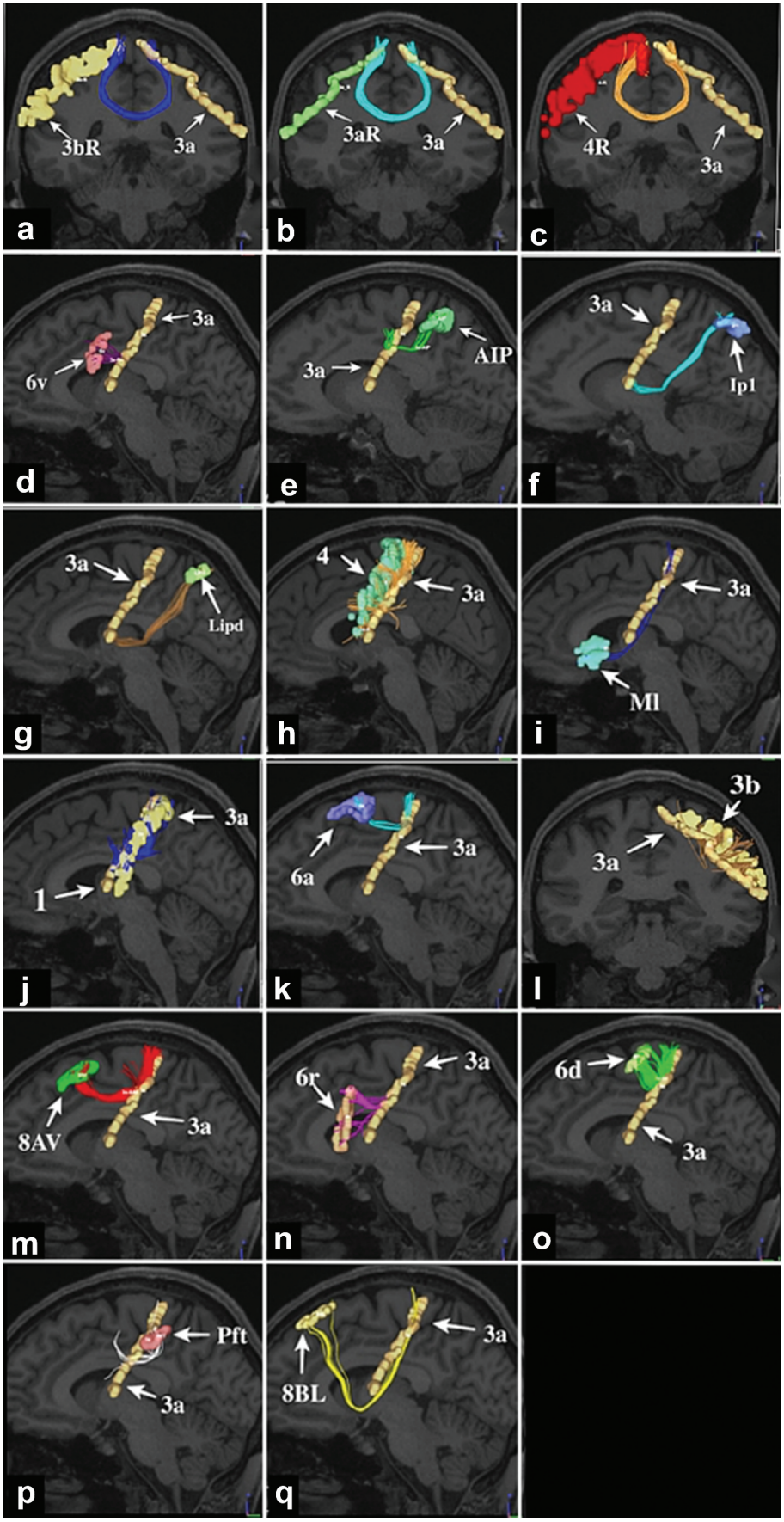

Figure 4. Diffusion tractography in sagittal and coronal planes showing connections of parcellations with area 3a. Different colors represent unique fiber bundle tracts.

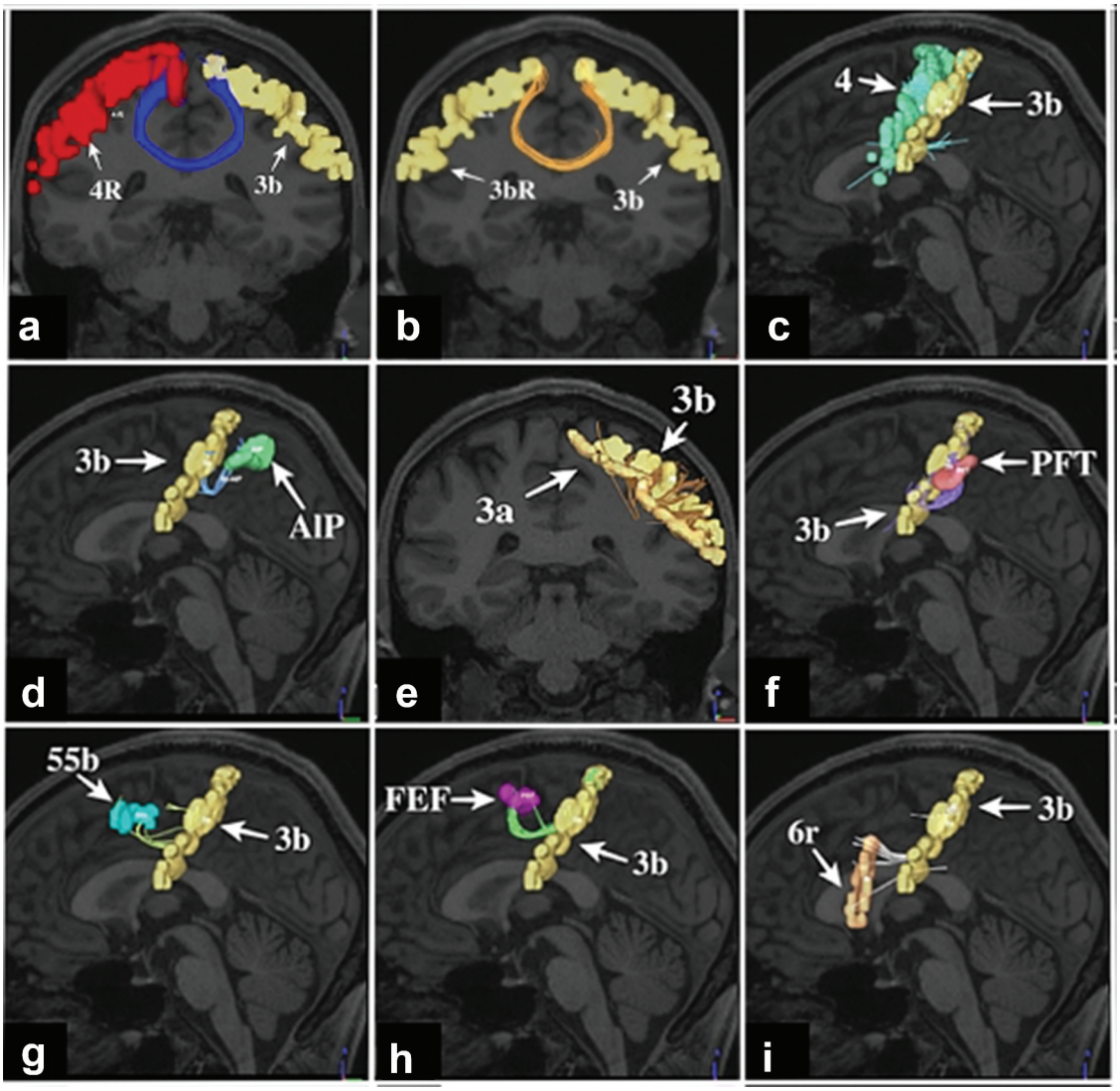

Figure 5. Diffusion tractography in sagittal and coronal planes showing connections of parcellations with area 3b. Different colors represent unique fiber bundle tracts.

Inferior and Superior Parietal Lobule

All parcellations within VPM were shown to have connectivity to portions of the Inferior Parietal Lobule (IPL). Area 3a of VPM showed connections to areas PFt and IPl of the IPL. Area 4 and area 3b of VPM showed connections to area PFt of IPL. Area 6v of VPM showed connections to area PFm of IPL. These connections can also be supported by functional similarities between the two regions considering IPL has been implicated in spatial perception and also the integration of visuomotor tasks [68]. These are skills related to the various functions of VPM, especially when considering its role in gripping and finger placement based on an object's size and shape [2–15]. Moreover, 6v was recently demonstrated to be part of the negative motor area of the face and upper limb [69].

Additionally, each VPM parcellation also showed connectivity to the areas of the Superior Parietal Lobule (SPL). Area 3a of VPM demonstrated connections to area LIPd of the SPL, and areas 3a, 3b, 4, and 6v each showed connections to area AIP of the SPL. Regions of the SPL have been suggested to function in visually guided motor tasks and also in creating an internal representation of one's whole body in space [70,71]. While the role of VPM in visuomotor tasks has been discussed previously, this is the first out of network connection that seems to possibly be contributing to action observation/imitation functionality seen by VPM [16–19] considering that such abilities would require some sort of proprioceptive input, likely being organized by and received from the ipsilateral SPL.

The VPM and DPM are two structurally and functionally different subregions and these differences may be related to their connections with the parietal and frontal regions [72]. The VPM has been previously described to be more interconnected with the IPL, and the DPM with the SPL. While we have also previously described connections between the DPM and the IPL and SPL [73], this current study did not

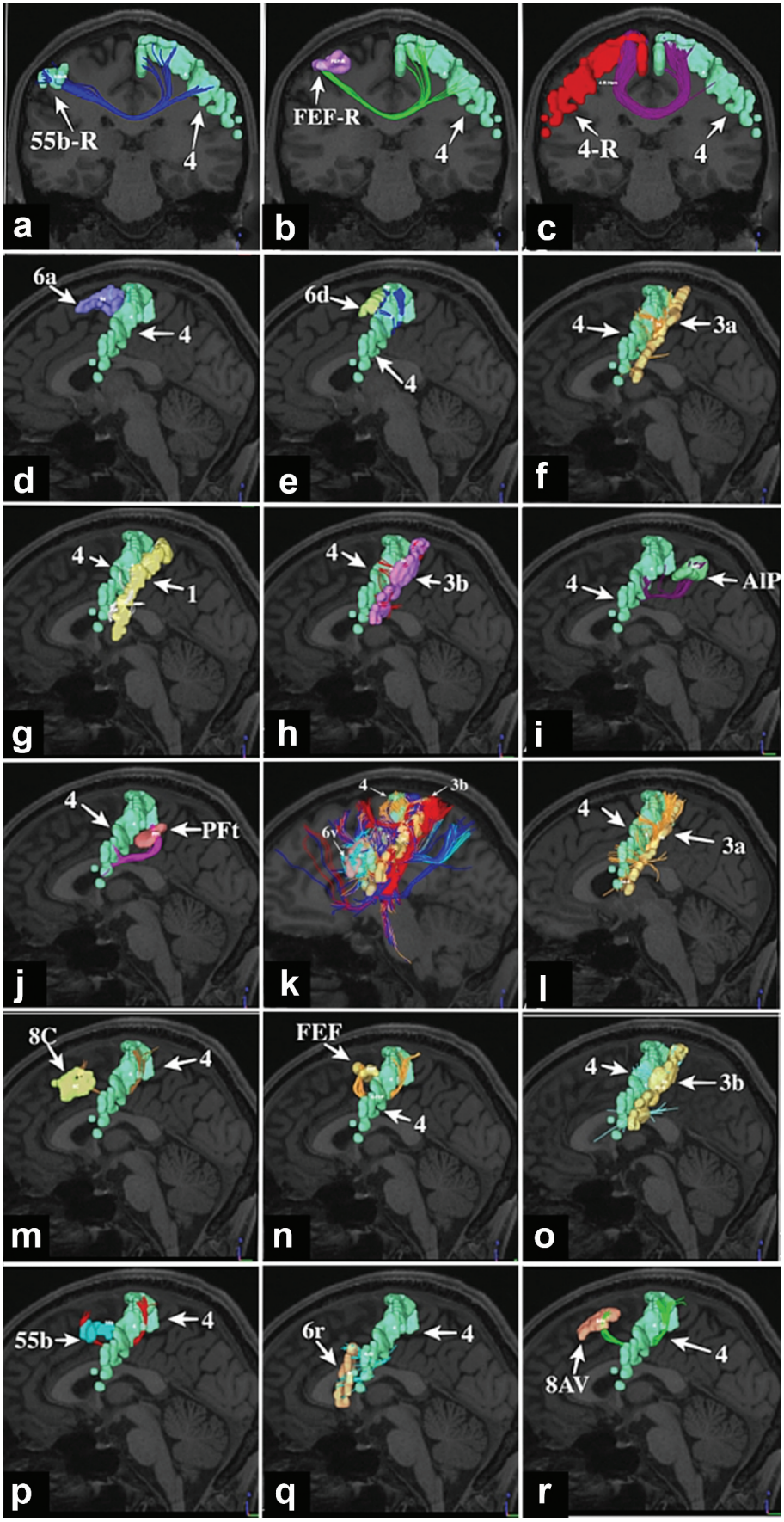

Figure 6. Diffusion tractography in sagittal and coronal planes showing connections of parcellations with area 4. Different colors represent unique fiber bundle tracts.

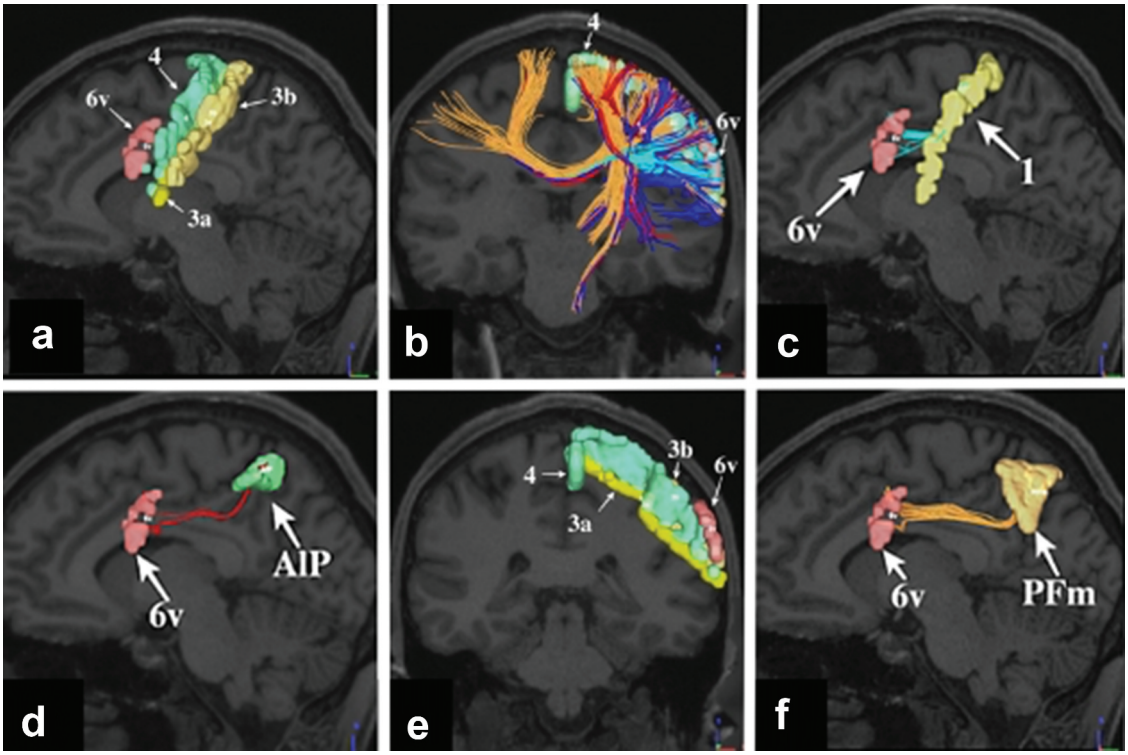

Figure 7. Diffusion tractography in sagittal and coronal planes showing connections of parcellations with area 6v. Different colors represent unique fiber bundle tracts.

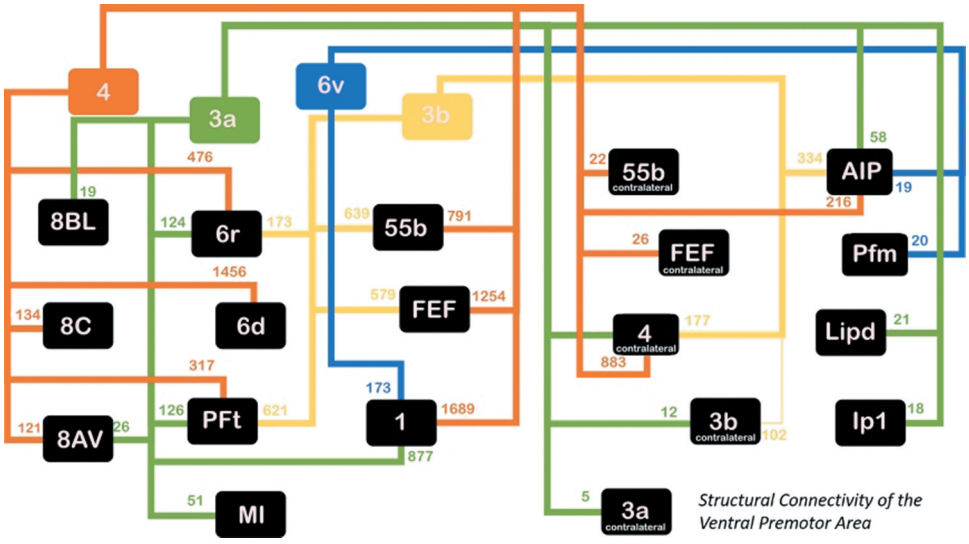

Figure 8. A wire schematic of the connections found in the study. The numbers indicate the average number of tracts between two cortical regions. Tract volumes were calculated as the average amount of tracts identified between cerebral hemispheres for each subject. All connections were to the ipsilateral brain region identified unless marked otherwise.

measure differences between the VPM and DPM with the parietal regions and offer an interesting opportunity for future study.

Sensorimotor

Areas 3a and 4 of VPM both showed connections to area 1 of the sensorimotor area. Area 1 is involved in the processing of cutaneous tactile stimulation from distal extremities. It provides not only input for the localization of such stimuli, but also characterizes the type of stimuli that is being experienced including information such as texture and nociception [74,75]. These are both important aspects of the known functions of the VPM especially when considering aspects of grasping movements [2–15]. Interestingly, all regions of interest in this study (area 4, 6v, 3b, and 3a) showed relatively strong connections to area 1, which were lateralized to the right (Table 1). Motor coordination, such as handedness, as well as painful and nonpainful somatosensory processing is commonly believed to be lateralized [4,76–78]. These

hemispheric asymmetries identified with area 1 could provide a possible covariate to include in future modeling of the mechanisms of handedness.

Insula

Area 3a of VPM shows connections to area MI near the insula. The insula is proposed to be involved in coordinating motor responses to relevant environmental stimuli [32,79]. While these functional connections are less clear between the two areas, it could be proposed that the insular white matter connections could contribute to the action observation/imitation functional role of VPM [15–18]. Additionally, it has also been shown that VPM can coordinate finger placement based on the geometrical shape of an object [3]. The geometrical shape may be one such environmental stimuli that require insular input to VPM. Furthermore, possible inter-hemispheric insular asymmetry was demonstrated as connections with MI from 3a were lateralized to the left, as described elsewhere [80]. Insular asymmetry favoring the left has been reported as early as in the neonate brain [81].

Limitations

Although our study provides an extensive model of cortical connections in the ventral premotor area, it was not without its limitations. Meta-analytic methodology provided this study the opportunity to study numerous cortical parcellations often previously studied in isolation; however, meta-analyses are inherently limited by the quality of literature [29]. We intended to be comprehensive in our definition of the VPM by using relevant region-based fMRIs to generate ALEs with a strict Cluster-Level Interference algorithm, but the analyzed studies still had differences in their methods and coordinate-based definitions of the VPM , which therefore inherently limits the quality of our data [82].

Furthermore, it is important to note that this manuscript was designed to be predominantly a qualitative, descriptive paper to provide anatomic information that encourages further study on functional relevance. Therefore, while connectomics allows the modeling of the common connections in an area of interest with strong prediction values [83], there are individual variations that may offer additional connections not readily apparent in connectomic analyses [84]. Still, connectomic analyses of large data sets allowed us the ability to observe possible relationships between cortical structures otherwise invisible to the human eye, such as the interhemispheric asymmetry identified between area 6v and 55b, which could provide insight into further study for future clinical applications. However, quantitative analyses from diffusion tractography should be viewed cautiously despite its ability to model qualitative analyses well due to limitations with individual uniqueness and differences.

Conclusions

We present a preliminary anatomical model of the ventral premotor area (VPM) and its connections within and outside of the motor system. Further studies may refine this model with the ultimate goal of clinical application.

Acknowledgments

Data was provided [in part] by the Human Connectome Project, WU-Minn Consortium (Principle Investigators: David Van Essen and Kamil Ugurbil; 1U54MH091657) funded by the 16 NIH Institutes and Centers that support the NIH Blueprint for Neuroscience Research; and by the McDonnell Center for Systems Neuroscience at Washington University.

Disclosure statement

Dr. Michael Sughrue is the Chief Medical Officer of Omniscient Neurotechnologies. No products directly related to this were discussed in this paper. The other authors report no conflict of interest concerning the materials or methods used in this study or the findings specified in this paper.

Funding

This study did not receive any funding to be completed.

Notes on contributors

John R. Sheets is an anesthesiology resident at the University of Oklahoma Health Sciences Center in Oklahoma, USA.

Robert G. Briggs is a neurosurgeon working at the University of Oklahoma Health Sciences Center in Oklahoma, USA.

Nicholas B. Dadario is a medical student pursuing a Doctor of Medicine degree at Rutgers Robert Wood Johnson Medical School in New Jersey, USA.

Isabella M. Young is a research associate at Cingulum Health in Sydney, Australia.

Michael Y. Bai is a student research assistant at Prince of Wales Private Hospital in Sydney, Australia.

Anujan Poologaindran is a neuroscience PhD student in the Brain Mapping Unit at the University of Cambridge and The Alan Turing Institute in the United Kingdom.

Cordell M. Baker is a neurosurgical resident at the University of Utah School of Medicine.

Andrew K. Conner is a neurosurgeon working at the University of California, San Francisco in California, USA.

Michael E. Sughrue is a neurosurgeon at the Prince of Wales Private Hospital and co-founder and Chief Medical Officer at Omniscient Neurotechnology, Sydney, Australia.

ORCID

Nicholas B. Dadario http://orcid.org/0000-0002-8657-187X
Isabella M. Young http://orcid.org/0000-0001-7639-6679
Michael Y. Bai http://orcid.org/0000-0002-5764-7740

References

[1] Hoshi E, Tanji J. A cortical parcellation-based analysis of ventral premotor area connectivity. Curr Opin Neurobiol. 2007;17(2):234–242. Epub 2007/ 02/24. PubMed PMID: 17317152.
[2] Davare M, Kraskov A, Rothwell JC, et al. Interactions between areas of the cortical grasping network. Curr Opin Neurobiol. 2011;21(4):565–570. Epub 2011/ 06/ 24. PubMed PMID: 21696944; PubMed Central PMCID: PMCPMC3437559.
[3] Dafotakis M, Sparing R, Eickhoff SB, et al. On the role of the ventral premotor cortex and anterior intraparietal area for predictive and reactive scaling of grip force. Brain Res. 2008;1228:73–80. Epub 2008/ 07/08. PubMed PMID: 18601912.
[4] Davare M, Andres M, Cosnard G, et al. Dissociating the role of ventral and dorsal premotor cortex in precision grasping. J Neurosci. 2006;26(8):2260–2268. Epub 2006/ 02/24. PubMed PMID: 16495453; PubMed Central PMCID: PMCPMC6674806.
[5] Cavina-Pratesi C, Monaco S, Fattori P, et al. Functional magnetic resonance imaging reveals the neural substrates of arm transport and grip formation in reach-to-grasp actions in humans. J Neurosci. 2010;30(31):10306–10323. PubMed PMID: 20685975. Epub 2010/ 08/06.
[6] Davare M, Lemon R, Olivier E. Selective modulation of interactions between ventral premotor cortex and primary motor cortex during precision grasping in humans. J Physiol. 2008;586(11):2735–2742. Epub 2008/ 04/12. PubMed PMID: 18403420; PubMed Central PMCID: PMCPMC2536583.
[7] Davare M, Montague K, Olivier E, et al. Ventral premotor to primary motor cortical interactions during object-driven grasp in humans. Cortex. 2009;45(9):1050–1057. Epub 2009/ 04/07. PubMed PMID: 19345344; PubMed Central PMCID: PMCPMC2730595.
[8] Prabhu G, Shimazu H, Cerri G, et al. Modulation of primary motor cortex outputs from ventral premotor cortex during visually guided grasp in the macaque monkey. J Physiol. 2009;587(5):1057–1069. PubMed PMID: 19139043; PubMed Central PMCID: PMCPMC2673775. Epub 2009/ 01/14.
[9] Davare M, Rothwell JC, Lemon RN. Causal connectivity between the human anterior intraparietal area and premotor cortex during grasp. Curr Biol. 2010;20(2):176–181. Epub 2010/ 01/26. PubMed PMID: 20096580; PubMed Central PMCID: PMCPMC2824111.
[10] Buch ER, Mars RB, Boorman ED, et al. A network centered on ventral premotor cortex exerts both facilitatory and inhibitory control over primary motor cortex during action reprogramming. J Neurosci. 2010;30(4):1395–1401. Epub 2010/ 01/29. PubMed PMID: 20107065; PubMed Central PMCID: PMCPMC2880444.
[11] Koch G, Cercignani M, Pecchioli C, et al. In vivo definition of parieto-motor connections involved in planning of grasping movements. Neuroimage. 2010;51(1):300–312. PubMed PMID: 20156564. Epub 2010/ 02/17.
[12] Dum RP, Strick PL. Frontal lobe inputs to the digit representations of the motor areas on the lateral surface of the hemisphere. J Neurosci. 2005;25(6):1375–1386. Epub 2005/ 02/11. PubMed PMID: 15703391.
[13] Ehrsson HH, Fagergren A, Jonsson T, et al. Cortical activity in precision- versus power-grip tasks: an fMRI study. J Neurophysiol. 2000;83(1):528–536. Epub 2000/ 01/15. PubMed PMID: 10634893.
[14] Ehrsson HH, Fagergren E, Forssberg H. Differential fronto-parietal activation depending on force used in a precision grip task: an fMRI study. J Neurophysiol. 2001;85(6):2613–2623. Epub 2001/ 06/02. PubMed PMID: 11387405.
[15] Kuhtz-Buschbeck JP, Ehrsson HH, Forssberg H. Human brain activity in the control of fine static precision grip forces: an fMRI study. Eur J Neurosci. 2001;14(2):382–390. PubMed PMID: 11553288. Epub 2001/ 09/13.
[16] Rizzolatti G, Fogassi L, Gallese V. Motor and cognitive functions of the ventral premotor cortex. Curr Opin Neurobiol. 2002;12(2):149–154. PubMed PMID: 12015230. Epub 2002/ 05/17.
[17] Johnson-Frey SH, Maloof FR, Newman-Norlund R, et al. Actions or hand-object interactions? Human inferior frontal cortex and action observation. Neuron. 2003;39(6):1053–1058. PubMed PMID: 12971903. Epub 2003/ 09/16.
[18] Binkofski F, Buccino G. The role of ventral premotor cortex in action execution and action understanding. J Physiol Paris. 2006;99(4–6):396–405. Epub 2006/ 05/26. PubMed PMID: 16723210.
[19] Morin O, Grezes J. What is "mirror" in the premotor cortex? A review. Neurophysiol Clin. 2008;38 (3):189–195. Epub 2008/ 06/10. PubMed PMID: 18539253.
[20] Glasser MF, Coalson TS, Robinson EC, et al. A multi-modal parcellation of human cerebral cortex. Nature. 2016;536(7615):171–178. PubMed PMID: 27437579; PubMed Central PMCID: PMCPMC4990127. Epub 2016/ 07/21.
[21] Turkeltaub PE, Eickhoff SB, Laird AR, et al. Minimizing within-experiment and within-group effects in activation likelihood estimation meta-analyses. Hum Brain Mapp. 2012;33(1):1–13. Epub 2011/ 02/10. PubMed PMID: 21305667; PubMed Central PMCID: PMCPMC4791073.
[22] Eickhoff SB, Laird AR, Grefkes C, et al. Coordinate-based activation likelihood estimation meta-analysis of neuroimaging data: a random-effects approach based on empirical estimates of spatial uncertainty. Hum Brain Mapp. 2009;30(9):2907–2926. Epub 2009/ 01/28. PubMed PMID: 19172646; PubMed Central PMCID: PMCPMC2872071.
[23] Fox PT, Lancaster JL. Opinion: mapping context and content: the BrainMap model. Nat Rev Neurosci. 2002;3(4):319–321. Epub 2002/ 04/23. PubMed PMID: 11967563.
[24] Fox PT, Laird AR, Fox SP, et al. BrainMap taxonomy of experimental design: description and evaluation. Hum Brain Mapp. 2005;25(1):185–198. PubMed PMID: 15846810. Epub 2005/ 04/23.

[25] Vanasse TJ, Fox PM, Barron DS, et al. BrainMap VBM: an environment for structural meta-analysis. Hum Brain Mapp. 2018;39(8):3308–3325. PubMed PMID: 29717540. Epub 2018/ 05/03.
[26] Laird AR, Lancaster JL, Fox PT. BrainMap: the social evolution of a human brain mapping database. Neuroinformatics. 2005;3(1):65–78. Epub 2005/ 05/ 18. PubMed PMID: 15897617.
[27] Grafton ST, Fadiga L, Arbib MA, et al. Premotor cortex activation during observation and naming of familiar tools. Neuroimage. 1997;6(4):231–236. Epub 1998/ 02/07. PubMed PMID: 9417966.
[28] Grafton ST, Hazeltine E, Ivry RB. Abstract and effector-specific representations of motor sequences identified with PET. J Neurosci. 1998;18(22):9420–9428. PubMed PMID: 9801380. Epub 1998/ 11/05.
[29] Stephan KM, Thaut MH, Wunderlich G, et al. Conscious and subconscious sensorimotor synchronization–prefrontal cortex and the influence of awareness. Neuroimage. 2002;15(2):345–352. PubMed PMID: 11798270. Epub 2002/ 01/19.
[30] Buccino G, Binkofski F, Fink GR, et al. Action observation activates premotor and parietal areas in a somatotopic manner: an fMRI study. Eur J Neurosci. 2001;13(2):400–404. Epub 2001/ 02/13 PubMed PMID: 11168545.
[31] Dassonville P, Lewis SM, Zhu XH, et al. The effect of stimulus-response compatibility on cortical motor activation. Neuroimage. 2001;13(1):1–14. Epub 2001/ 01/03. PubMed PMID: 11133304.
[32] Ehrsson HH, Naito E, Geyer S, et al. Simultaneous movements of upper and lower limbs are coordinated by motor representations that are shared by both limbs: a PET study. Eur J Neurosci Epub 2000/ 09/ 21. 2000;12(9):3385–3398. PubMed PMID: 10998121.
[33] Wheaton KJ, Thompson JC, Syngeniotis A, et al. Viewing the motion of human body parts activates different regions of premotor, temporal, and parietal cortex. Neuroimage. 2004;22(1):277–288. Epub 2004/ 04/28. PubMed PMID: 15110018.
[34] Johnson-Frey SH, Newman-Norlund R, Grafton ST. A distributed left hemisphere network active during planning of everyday tool use skills. Cereb Cortex. 2005;15(6):681–695. Epub 2004/ 09/03. PubMed PMID: 15342430; PubMed Central PMCID: PMCPMC1364509.
[35] Creem-Regehr SH, Lee JN. Neural representations of graspable objects: are tools special? Brain Res Cogn Brain Res. 2005;22(3):457–469. Epub 2005/ 02/22. PubMed PMID: 15722215.
[36] Leslie KR, Johnson-Frey SH, Grafton ST. Functional imaging of face and hand imitation: towards a motor theory of empathy. Neuroimage. 2004;21(2):601–607. Epub 2004/ 02/26. PubMed PMID: 14980562.
[37] Stephan KM, Fink GR, Passingham RE, et al. Functional anatomy of the mental representation of upper extremity movements in healthy subjects. J Neurophysiol. 1995;73 (1):373–386. PubMed PMID: 7714579. Epub 1995/ 01/01.
[38] Dresel C, Castrop F, Haslinger B, et al. The functional neuroanatomy of coordinated orofacial movements: sparse sampling fMRI of whistling. Neuroimage. 2005;28(3):588–597. Epub 2005/ 08/09. PubMed PMID: 16084116.
[39] Isaev G, Murphy K, Guz A, et al. Areas of the brain concerned with ventilatory load compensation in awake man. J Physiol. 2002;539(3):935–945. PubMed PMID: 11897862; PubMed Central PMCID: PMCPMC2290189. Epub 2002/ 03/19.
[40] Ghosh SS, Tourville JA, Guenther FH. A neuroimaging study of premotor lateralization and cerebellar involvement in the production of phonemes and syllables. J Speech Lang Hear Res. 2008;51(5):1183–1202. Epub 2008/ 07/31. PubMed PMID: 18664692; PubMed Central PMCID: PMCPMC2652040.
[41] Cross ES, Hamilton AF, Grafton ST. Building a motor simulation de novo: observation of dance by dancers. Neuroimage. 2006;31(3):1257–1267. Epub 2006/ 03/ 15. PubMed PMID: 16530429; PubMed Central PMCID: PMCPMC1821082.
[42] Montgomery KJ, Isenberg N, Haxby JV. Communicative hand gestures and object-directed hand movements activated the mirror neuron system. Soc Cogn Affect Neurosci. 2007;2(2):114–122. Epub 2008/ 11/06. PubMed PMID: 18985130; PubMed Central PMCID: PMCPMC2555455.
[43] Pa C, M-e L, Ec C, et al. Dissociable neural mechanisms for determining the perceived heaviness of objects and the predicted weight of objects during lifting: an fMRI investigation of the size–weight illusion. Neuroimage. 2009;44(1):200–212.
[44] Monaco S, Sedda A, Cavina-Pratesi C, et al. Neural correlates of object size and object location during grasping actions. Eur J Neurosci. 2015;41(4):454–465. Epub 2014/ 11/18. PubMed PMID: 25400211.
[45] Lotze M, Heymans U, Birbaumer N, et al. Differential cerebral activation during observation of expressive gestures and motor acts. Neuropsychologia. 2006;44 (10):1787–1795. PubMed PMID: 16730755. Epub 2006/ 05/30.
[46] Colebatch JG, Deiber MP, Passingham RE, et al. Regional cerebral blood flow during voluntary arm and hand movements in human subjects. J Neurophysiol. 1991;65(6):1392–1401. Epub 1991/ 06/01. PubMed PMID: 1875248.
[47] Winstein CJ, Grafton ST, Pohl PS. Motor task difficulty and brain activity: investigation of goal-directed reciprocal aiming using positron emission tomography. J Neurophysiol. 1997;77(3):1581–1594. Epub 1997/ 03/ 01. PubMed PMID: 9084621.
[48] Boecker H, Ceballos-Baumann AO, Bartenstein P, et al. A H(2)(15)O positron emission tomography study on mental imagery of movement sequences–the effect of modulating sequence length and direction. Neuroimage Epub 2002/ 10/16. 2002;17 (2):999–1009. PubMed PMID: 12377173.
[49] Sadato N, Campbell G, Ibanez V, et al. Complexity affects regional cerebral blood flow change during sequential finger movements. J Neurosci. 1996;16 (8):2691–2700. PubMed PMID: 8786445. Epub 1996/ 04/15.
[50] Cunnington R, Windischberger C, Robinson S, et al. The selection of intended actions and the observation of others' actions: a time-resolved fMRI study. Neuroimage. 2006;29(4):1294–1302. Epub 2005/ 10/ 26. PubMed PMID: 16246592.
[51] Chen JL, Rae C, Watkins KE. Learning to play a melody: an fMRI study examining the formation of auditory-motor associations. Neuroimage. 2012;59(2):1200–1208. Epub 2011/ 08/30. PubMed PMID: 21871571.
[52] Aramaki Y, Honda M, Okada T, et al. Neural correlates of the spontaneous phase transition during bimanual coordination. Cereb Cortex. 2006;16(9):1338–1348. Epub 2005/ 11/25. PubMed PMID: 16306323.
[53] Kuhtz-Buschbeck JP, Mahnkopf C, Holzknecht C, et al. Effector-independent representations of simple and

complex imagined finger movements: a combined fMRI and TMS study. Eur J Neurosci. 2003;18(12):3375–3387. PubMed PMID: 14686911. Epub 2003/ 12/23.

[54] Haslinger B, Erhard P, Weilke F, et al. The role of lateral premotor–cerebellar–parietal circuits in motor sequence control: a parametric fMRI study. Cognit Brain Res. 2002;13(2):159–168.

[55] Jancke L, Loose R, Lutz K, et al. Cortical activations during paced finger-tapping applying visual and auditory pacing stimuli. Brain Res Cogn Brain Res. 2000;10(1–-2):51–66. PubMed PMID: 10978692. Epub 2000/ 09/09.

[56] Larsson J, Gulyas B, Roland PE. Cortical representation of self-paced finger movement. Neuroreport. 1996;7(2):463–468. PubMed PMID: 8730806. Epub 1996/ 01/31.

[57] Sotiropoulos SN, Jbabdi S, Xu J, et al. Advances in diffusion MRI acquisition and processing in the human connectome project. Neuroimage. 2013;80:125–143. Epub 2013/ 05/25. PubMed PMID: 23702418; PubMed Central PMCID: PMCPMC3720790.

[58] Yeh F, Wedeen VJ, Tseng WI. Generalized ${q}$-Sampling Imaging. IEEE Trans Med Imaging. 2010;29(9):1626–1635.

[59] De Schotten MT, Dell'Acqua F, Forkel SJ, et al. A lateralized brain network for visuospatial attention. Nat Neurosci. 2011;14(10):1245–1246.

[60] Fulton JF. A note on the definition of the "motor" and "premotor" areas. Brain. 1935;58(2):311–316.

[61] Hopf A. Distribution of myeloarchitectonic marks in the frontal cerebral cortex in man. J Hirnforsch. 1956;2(4):311–333. Epub 1956/ 01/01. PubMed PMID: 13376888.

[62] Amunts K, Zilles K. Architecture and organizational principles of Broca's region. Trends Cogn Sci. 2012;16(8):418–426.

[63] Crowne DP. The frontal eye field and attention. Psychol Bull. 1983;93(2):232.

[64] Costafreda SG, Fu CH, Lee L, et al. A systematic review and quantitative appraisal of fMRI studies of verbal fluency: role of the left inferior frontal gyrus. Hum Brain Mapp. 2006;27(10):799–810. Epub 2006/ 03/03. PubMed PMID: 16511886.

[65] Poldrack RA, Wagner AD, Prull MW, et al. Functional specialization for semantic and phonological processing in the left inferior prefrontal cortex. Neuroimage. 1999;10(1):15–35. Epub 1999/ 07/01. PubMed PMID: 10385578.

[66] Swick D, Ashley V, Turken AU. Left inferior frontal gyrus is critical for response inhibition. BMC Neurosci. 2008;9(1):102. Epub 2008/ 10/23. PubMed PMID: 18939997; PubMed Central PMCID: PMCPMC2588614.

[67] Talati A, Hirsch J. Functional specialization within the medial frontal gyrus for perceptual go/no-go decisions based on "what," "when," and "where" related information: an fMRI study. J Cogn Neurosci. 2005;17(7):981–993. Epub 2005/ 08/17. PubMed PMID: 16102231.

[68] Andersen RA. Inferior parietal lobule function in spatial perception and visuomotor integration. Compr Physiol. 2011;483-518.

[69] Rech F, Herbet G, Gaudeau Y, et al. A probabilistic map of negative motor areas of the upper limb and face: a brain stimulation study. Brain. 2019;142(4):952–965. PubMed PMID: 30753319; PubMed Central PMCID: PMCPMC6439333. Epub 2019/ 02/13.

[70] Wolpert DM, Goodbody SJ, Husain M. Maintaining internal representations: the role of the human superior parietal lobe. Nat Neurosci. 1998;1(6):529–533.

[71] Wang J, Yang Y, Fan L, et al. Convergent functional architecture of the superior parietal lobule unraveled with multimodal neuroimaging approaches. Hum Brain Mapp. 2015;36(1):238–257. PubMed PMID: 25181023; PubMed Central PMCID: PMCPMC4268275. Epub 2014/ 09/03.

[72] Tomassini V, Jbabdi S, Klein JC, et al. Diffusion-weighted imaging tractography-based parcellation of the human lateral premotor cortex identifies dorsal and ventral subregions with anatomical and functional specializations. J Neurosci. 2007;27(38):10259–10269. PubMed PMID: 17881532; PubMed Central PMCID: PMCPMC6672665. Epub 2007/ 09/21.

[73] Sheets JR, Briggs RG, Bai MY, et al. Parcellation-based modeling of the dorsal premotor area. J Neurol Sci. 2020;415:116907.

[74] Ploner M, Schmitz F, Freund HJ, et al. Differential organization of touch and pain in human primary somatosensory cortex. J Neurophysiol. 2000;83(3):1770–1776. Epub 2000/ 03/11. PubMed PMID: 10712498.

[75] Vierck CJ, Whitsel BL, Favorov OV, et al. Role of primary somatosensory cortex in the coding of pain. Pain. 2013;154(3):334–344. Epub 2012/ 12/19. PubMed PMID: 23245864; PubMed Central PMCID: PMCPMC4501501.

[76] Schlerf JE, Galea JM, Spampinato D, et al. Laterality differences in cerebellar–motor cortex connectivity. Cereb Cortex. 2014;25(7):1827–1834.

[77] Coghill RC, Gilron I, Iadarola MJ. Hemispheric lateralization of somatosensory processing. J Neurophysiol. 2001;85(6):2602–2612. Epub 2001/ 06/02. PubMed PMID: 11387404.

[78] Sainburg RL. Convergent models of handedness and brain lateralization. Front Psychol. 2014;5(1092). doi:10.3389/fpsyg.2014.01092

[79] Menon V, Uddin LQ. Saliency, switching, attention and control: a network model of insula function. Brain Struct Funct. 2010;214(5–6):655–667. Epub 2010/ 06/01. PubMed PMID: 20512370; PubMed Central PMCID: PMCPMC2899886.

[80] Van Essen DC, Glasser MF, Dierker DL, et al. Parcellations and hemispheric asymmetries of human cerebral cortex analyzed on surface-based atlases. Cereb Cortex. 2012;22(10):2241–2262. Epub 2011/ 11/04. PubMed PMID: 22047963; PubMed Central PMCID: PMCPMC3432236.

[81] Ratnarajah N, Rifkin-Graboi A, Fortier MV, et al. Structural connectivity asymmetry in the neonatal brain. Neuroimage. 2013;75:187–194. Epub 2013/ 03/19. PubMed PMID: 23501049; PubMed Central PMCID: PMCPMC3959921.

[82] Tench CR, Tanasescu R, Auer DP, et al. Coordinate based meta-analysis of functional neuroimaging data; false discovery control and diagnostics. Plos One. 2013;8(7):e70143.

[83] Finn ES, Shen X, Scheinost D, et al. Functional connectome fingerprinting: identifying individuals using patterns of brain connectivity. Nat Neurosci. 2015;18(11):1664–1671. PubMed PMID: 26457551. Epub 2015/ 10/12.

[84] Melozzi F, Bergmann E, Harris JA, et al. Individual structural features constrain the mouse functional connectome. Proc Nat Acad Sci. 2019;116(52):26961.